Molecular Nutrition & Food Research
www.mnf-journal.com

The Protective Effect of Pumpkin and Fermented Whey Mixture against AFB1 and OTA Immune Toxicity In Vitro. A Transcriptomic Approach

Massimo Frangiamone, Manuel Lozano, Alessandra Cimbalo, Alvaro Lazaro, Guillermina Font, and Lara Manyes*

Scope: The aim of the study is to investigate in Jurkat cells the possible beneficial effect of pumpkin (P) and fermented milk whey (FW) mixture against aflatoxin B1 (AFB1) and ochratoxin A (OTA) induced alterations in gene expression profile.

Methods and results: Human T cells are exposed for 7 days to digested bread extracts containing P-FW mixture along with AFB1 and OTA, individually and in combination. The results of RNA sequencing show that AFB1 P-FW exposure resulted in 34 differentially expressed genes (DEGs) while 3450 DEGs are found in OTA P-FW exposure and 3264 DEGs in AFB1-OTA P-FW treatment. Gene ontology analysis reveals biological processes and molecular functions related to immune system and inflammatory response. Moreover, PathVisio analysis points to eicosanoid signaling via lipoxygenase as the main pathway altered by AFB1 P-FW exposure whereas interferon signaling is the most affected pathway after OTA P-FW and AFB1-OTA P-FW treatments.

Conclusions: The mitigation of genes and inherent pathways typically associated with the inflammatory response suggest not only the anti-inflammatory and protective role of P-FW mixture but also their possible application in food industry to counteract AFB1 and OTA toxic effects on human and animal health.

1. Introduction

Aflatoxin B1 (AFB1) is a polyketide compound synthesized by *Aspergillus flavus* and *Aspergillus parasiticus*, which toxic effects have been reported in liver, kidney, brain, and immune system. Thus, AFB1 has been classified by the International Agency for Research on Cancer (IARC) in the group 1 as human carcinogen.[1] This mycotoxin is commonly found in cereals, oil seeds, dried fruits, spices, milk, and meat. In order to protect human health, the European Union (EU) sets the maximum tolerable limits of AFB1 at 2–5 μg kg^{-1} in cereals, 5 μg kg^{-1} in spices, 2–8 μg kg^{-1} in dried fruits, 6 μg kg^{-1} in dietary foods for medical purpose, and 0.1 μg kg^{-1} in foods for infants and young children.[2]

Another widespread mycotoxin, ochratoxin A (OTA), is mainly produced by *Penicillium* and *Aspergillus* species. Several studies have demonstrated that OTA-exposure can elicit nephrotoxicity and immune toxicity in vitro and in vivo. Hence, IARC has classified OTA in the group 2B as possibly carcinogenic to humans.[3] Typical foods contaminated by OTA are cereals, wine, spices, meat, and dried fruits. The EU established the maximum tolerable levels of OTA at 5 μg kg^{-1} in unprocessed cereals, 8 μg kg^{-1} in wheat gluten, 10 μg kg^{-1} in soluble coffee, 15 μg kg^{-1} in spices, 2 μg kg^{-1} in grape juice and wine whereas in infants and dietary foods for medical purpose at 0.5 μg kg^{-1}.[2]

Mycotoxin bioaccessibility is one of the main aspects to take into account for human health risk assessment. Although AFB1 and OTA are found in a wide range of food commodities, cereals and cereal-based products are the main foods to be contaminated.[4,5] Accordingly, AFB1 and OTA bioaccessibility was widely assessed in cereals by using in vitro human digestion models. In relation to AFB1, high values of intestinal bioaccessibility were obtained. In detail, values of 87% in wheat, 88–92% in maize, 95% in corn, and 114% in bread were detected.[6,7–9] Regarding OTA, values of 100% in buckwheat, 99% in cereal-based foods, and 38–88% in bread were observed.[8,10–12] Once absorbed, AFB1 and OTA can trigger an innate and adaptive response by the immune system. In detail, the innate immune response involves physical barriers, such as epithelial cell layers, along with proteins and bioactive small molecules that are constitutively present in biological fluids (defensins and ficolins) or released by immune cells once activated (cytokines and

M. Frangiamone, M. Lozano, A. Cimbalo, A. Lazaro, G. Font, L. Manyes
Laboratory of Food Chemistry and Toxicology
Faculty of Pharmacy
Universitat de València
Av. Vicent Andrés Estellés s/n, Burjassot 46100, Spain
E-mail: alessandra.cimbalo@uv.es

The ORCID identification number(s) for the author(s) of this article can be found under https://doi.org/10.1002/mnfr.202200902

DOI: 10.1002/mnfr.202200902

chemokines). In addition, various immune cell types such as neutrophils, eosinophils, basophils, and macrophages play a key role in identifying and eliminating pathogens. Conversely, the adaptive immune response is more specific and involves T and B lymphocytes, which are responsible for recognizing and scavenging pathogen-infected cells. Among lymphocytes, it is important to mention memory T cells, which immediately become active in case pathogens reinfect the organism.[13] Recent studies demonstrated that exposure to AFB1 and OTA exhibited toxic effects on the innate and adaptive response by disrupting epithelial defense barriers and altering the proliferation, differentiation, or maturation of lymphocytes, dendritic cells, and macrophages. In cellular and animal models, AFB1 and OTA can also induce a state of immunosuppression accompanied by chronic inflammation, which is related to the onset of severe systemic diseases.[14–17]

On the other hand, food processing and innovative technologies can reduce mycotoxin contamination by promoting its degradation, even though the risk to humans cannot be eliminated.[18] Therefore, the use of bioactive compounds has been recently proposed as a new food strategy to reduce mycotoxins absorption and prevent their systemic effects on human and animal health.[8] Pumpkin, which belongs to *Cucurbitaceae* family, is rich in carotenoids (β-carotene, lutein, lycopene, and zeaxanthin) that play an important role to protect cells from oxidative stress and damage, preventing the onset of several human diseases.[19] Milk whey, a cheese by-product with high nutritional values, is an excellent source of functional compounds, such as antifungal peptides, and an optimal substrate for lactic acid bacteria (LAB) fermentation.[20]

The addition of these functional ingredients in bread formulation improved its shelf life, inhibited the growth of mycotoxigenic fungi, reduced AFB1 and OTA production as well as their intestinal bioaccessibility.[21,22] Escrivá et al.[8] showed how the introduction of pumpkin (P) in bread preparation significantly reduced bioaccessibility values by up to 74% for AFB1 and 34% for OTA. Fermented whey (FW) and the combination of P-FW showed intestinal bioaccessibility reductions between 57% and 68% for AFB1, and between 11% and 20% for OTA. A large reduction of bioaccessibility value by up to 95% was also observed for both toxins after including specific LAB strains in contaminated breads.[9,12] Carotenoids and FW-derived bioactive compounds also reported high in vitro bioavailability values (10–60% and 10–22%, respectively), thus showing the ability to reach the bloodstream and potentially exert a systemic effect.[23,24] The beneficial role of pumpkin has been also proved at mitochondrial transcriptional level after AFB1 and OTA exposure in a blood-brain barrier in vitro model.[25,26] FW-derived bioactive compounds can also inhibit AFB1 and OTA production and toxicity in vitro.[27] Furthermore, it is interesting to emphasize the synergistic and additive effect of P and FW in vitro and in vivo. In SH-SY5Y cells, the addition of P-FW mixture in AFB1 and OTA contaminated breads not only enhanced the expression of typical neuronal differentiation markers, but also attenuated cell cycle alterations and improved the overall gene expression impaired by mycotoxins exposure.[28] In spontaneously hypertensive rats, the administration of pumpkin pectin and milk whey mixture improved blood pressure and gut microbiota dysbiosis.[29]

In this context, the scientific community developed several technologies to thoroughly investigate not only mycotoxins mode of action but also the protective role of bioactive compounds. For instance, *-omics* techniques such as genomics, transcriptomics, proteomics, and metabolomics represent one of the most useful tools in toxicology research as these assays enable to understand how toxic molecules can disrupt the structure, function, and dynamics of a cell, tissue, and organism. In particular, next generation sequencing (NGS) is a very powerful, highly sensitive, and accurate high-throughput sequencing approach that provides comprehensive and speedy gene expression profiles. In addition, NGS technology can be employed to gain further insight into cell responses, gene expression changes, and signaling pathways activation related to specific contaminants.[30,31]

Therefore, the aim of the present study was to evaluate the potential effect of P-FW mixture against AFB1 and OTA promoted immune toxicity at transcriptional level in human lymphoblastic Jurkat cells by using digested bread extracts.

2. Experimental Section

2.1. Reagents

The reagents and cell culture compounds used: Roswell Park Memorial Institute (RPMI)-glutamax medium, Fetal Bovine Serum (FBS), penicillin/streptomycin and phosphate buffer saline were purchased by Sigma Chemical Co. (St. Louis, MO, USA) while methanol was acquired from Fisher Scientific (Madrid, Spain). Deionized water (<18 MΩ cm resistivity) was obtained by Milli-QSP Reagent Water System (Millipore, Bedford, MA, USA). Natural ingredients for bread preparation: pumpkin, wheat flour, mineral water, salt (NaCl), and sugar (sucrose) were acquired from a commercial supermarket (Valencia, Spain). Goat milk whey coagulated by commercial rennet (starter culture R-604) was purchased from ALCLIPOR society (Benassal, Spain) while LAB used in this study (*Lactobacillus plantarum CECT 220*) was obtained from CECT (Paterna, Valencia, Spain).

2.2. Cell Culture and Treatments Exposure

Jurkat cells (ATCC TIB-152) derived from human T lymphocytes peripheral blood were maintained in RPMI-glutamax medium supplemented with 100 U mL^{-1} penicillin, 100 mg mL^{-1} streptomycin, and 10% FBS. The incubation conditions were pH 7.4, 5% CO_2 at 37 °C, and 95% air atmosphere at constant humidity. The medium was changed every 2–3 days. To achieve the goal of the study, Jurkat cells were seeded at a density of 3×10^5 cells mL^{-1} in six well plates and treated for 7 days with bread extracts obtained after a simulated in vitro human digestion. These digested extracts, containing the combination of P and FW (both at 1% w/w) along with mycotoxins (AFB1, OTA, and their combination), were added to the culture medium using a final dilution of 1:10. **Table 1** showed the average concentration and profile of carotenoids identified in digested bread extracts using the method described by Juan et al.[20] **Table 2** showed AFB1 and OTA concentrations in digested bread extracts once diluted. Mycotoxins doses were determined as explained by Escrivá et al.[8]

Table 1. Average concentration (μg mL^{-1}) and profile of carotenoids identified in digested bread extracts.

	Carotenoids concentration [μg mL^{-1}]					
Bread	β-carotene	Lutein	Antheraxanthin	Violaxanthin	Zeaxanthin	β-cryptoxanthin
P-FW	1.8636	0.0180	n.d.	3.3676	n.d.	2.9880
AFB1 P-FW	2.5152	0.0122	0.0054	3.0368	0.0054	2.3976
OTA P-FW	4.0000	0.0120	n.d.	3.3971	n.d.	2.3614
AFB1-OTA P-FW	2.2879	0.0086	0.0580	2.7426	0.0580	1.8554

n.d., not detected.

Table 2. AFB1 and OTA concentrations in digested bread extracts after a dilution of 1:10.

Treatment	AFB1 [nM]	OTA [nM]
P-FW	-	-
AFB1 P-FW	196	-
OTA P-FW	-	1037
AFB1-OTA P-FW	187	837

2.3. RNA Extraction and Next Generation Sequencing (NGS)

Total RNA of the control and treated Jurkat cells was isolated through ReliaPrep RNA Cell Miniprep System Kit (Promega, USA) and purified to remove genomic DNA contamination. The RNA extracted from each sample was checked for quantity and quality using a NeoDot UV/vis Nano Spectrophotometer (Quimigen, Madrid, Spain) showing appropriate 260/280 and 260/230 nm ratios both around 2. All sequenced samples were generated from high quality RNA samples having an RNA integrity number >8. The standard Illumina protocol was followed to develop RNA-seq libraries, using TruSeq stranded mRNA. Then, Illumina NextSeq 500 platform was employed for sequencing. RNA-seq data acquisition, which consisted of several steps from raw reads to read alignment and quantification, was specifically checked at each step. The percentage of mapped reads, which indicated high sequencing accuracy and low presence of contaminating DNA was calculated by FastQC version 0.11.8.[26] Afterwards, one archive for each sample was obtained, 12 in total. RNA quality control and sequencing were performed by the Genomics section of the Central Service for Experimental Research (SCSIE, University of Valencia, Valencia, Spain).

2.4. Data Processing

The quality control (QC) of reads was performed by FastQC software v0.11.8.[32] The trimming was performed with FASTX-Toolkit v0.13, discarding the low-quality bases from 5'- and 3'-extremes.[33] Then, low quality reads and the identical sequences found in each file were collapsed into a single sequence while reads counts were maintained. The trimmed reads alignment was carried out by Spliced Transcripts Alignment to a Reference (STAR) software v2.7, using as reference the Genome Reference Consortium Human Build 38 version.[34] The Sequence Alignment Map (SAM) files were transformed in their binary version (BAM), ordered and indexed by SAM tools software v1.10.[35] BAM files were used with STAR to generate an expression matrix in *R* software.[36] Annotation, normalization, and statistical analysis to contrast differential expression between treatments and control were carried out according to the user guide of *edgeR* package, by using gene-wise negative binomial generalized linear models with quasi-likelihood tests.[37] Differentially expressed genes (DEGs) with p-value ≤0.05 were considered significant. Gene expression compared to the control was expressed as the logarithm of the fold change (log2FC). Diagrams and heat maps were plotted by *Vennerable* and *pheatmap* packages assessing coincident DEGs between conditions.[38–41]

2.5. Gene Expression Analysis

The selected DEGs were submitted to over-representation and gene ontology (GO) analysis by DAVID bioinformatics resources in order to obtain GO annotations and functional DEGs classifications.[42,43] Pathway assignments were carried out through PathVisio software using WikiPathways as biological pathways database,[44,45] Z-score > 1.96 and adj. $p \leq 0.05$ were used as thresholds to identify significant pathways.

2.6. Gene Selection and Primer Design

Gene-specific primers were designed by Primer-BLAST using the default software settings and with amplified PCR products ranging from 203 to 228 bp and T_m at 57–60 °C. Standard curves by qPCR were performed for all primers and a single amplification product for each gene was obtained by the melting curve assay in StepOne Plus Real-time PCR instrument (Applied Biosystems, CA, USA). Primer amplification efficiency was determined from the standard curve generated by serial dilution of cDNA (five fold each) for each gene. Correlation coefficient (R^2 values; i.e., linearity) and amplification efficiencies were calculated from the slope of the regression line by plotting Ct mean values against the log cDNA dilution factor. The gene-specific primers used in the present study were listed in **Table 3**.

2.7. Reverse Transcription and qPCR

Also for qPCR analysis, total RNA of the control and exposed cells was isolated using ReliaPrep RNA Cell Miniprep System Kit (Promega, USA) and purified to remove genomic DNA contamination. The RNA extracted from each sample was checked

Table 3. Gene names, forward and reverse primer sequences, PCR efficiency, and linearity value for the target genes and the reference gene GAPDH.

Gene	Primer forward sequence	Primer reverse sequence	Efficiency [%]	Linearity
GAPDH	GGAGTCCACTGGCGTCTT	GAGTCCTTCCACGATACCAAA	110	0.991
RHOB	TCGTGTTCAGTAAGGACGAG	ACTTCTCGGGGATGTTCTC	108	0.996
TIGD5	TGGAGCCACCTGACTTACCT	AGAACCAGGGTTTGACAGGC	94	0.990

for quantity and quality using a NeoDot UV/vis Nano Spectrophotometer (Quimigen, Madrid, Spain) showing concentrations around 500 ng μL^{-1} along with appropriate 260/280 and 260/230 nm ratios both around 2. RNA samples were diluted to 100 ng μL^{-1} with sterilized Milli-Q H_2O and cDNA was then synthesized by TaqMan Reverse Transcription Kit (Applied Biosystems). Real-time amplification reactions were performed in 96 well plates using SYBR Green detection chemistry and were run in triplicate by StepOne Plus Real-time PCR instrument (Applied Biosystems, CA, USA). Reactions were prepared as follows: 100 ng of template, 500 nM of each primer, the required amount of 2× Fast SYBR Green in a reaction volume of 10 µL. The PCR temperature cycling conditions for Ras Homolog Family Member B (RHOB) and Tigger Transposable Element Derived 5 (TIGD5) were as follows: initial denaturation step at 95 °C for 5 min to activate Taq DNA polymerase, followed by 40 cycles of denaturation at 95 °C for 10 s, annealing at 60 °C for 30 s, and elongation at 72 °C for 15 s. The melting curve was generated by heating the amplicon from 60 to 90 °C. Threshold cycles (Ct) and relative quantification (RQ) were automatically generated by StepOne Plus Software version 2.3. Experiments were carried out in triplicate according to Minimum Information for Publication of Quantitative Real-Time PCR Experiments (MIQE) guidelines.[46]

2.8. Statistical Analysis

In RNA-seq, the statistical analysis was carried out using *R* statistical package version 3.5.1[36] while in qPCR analysis, statistics were performed by ΔCt values (experimental Ct – housekeeping Ct mean) obtained by StepOne Plus Software version 2.3. Group variances were assessed by Levene's test and all group variances were equal. Differences between groups were defined by *t*-student test. In all cases, a p value ≤0.05 was considered for statistically significant differences.

3. Results

3.1. Gene Expression Profile

The overall gene expression of Jurkat cells treated during 7 days with AFB1 P-FW, OTA P-FW, and AFB1-OTA P-FW significantly differed from the control. Using a p-value ≤ 0.05 and log2FC |1.0|, AFB1 P-FW exposure resulted in 34 DEGs with 23 up- and 11 downregulated, 3450 DEGs (2135 up- and 1315 downregulated) were found in OTA P-FW exposure and 3264 DEGs (2050 up- and 1214 downregulated) in the combined treatment. Considering all conditions, the total number of DEGs was 6748 with 62.3% upregulation and 37.7% downregulation, compromising the usual

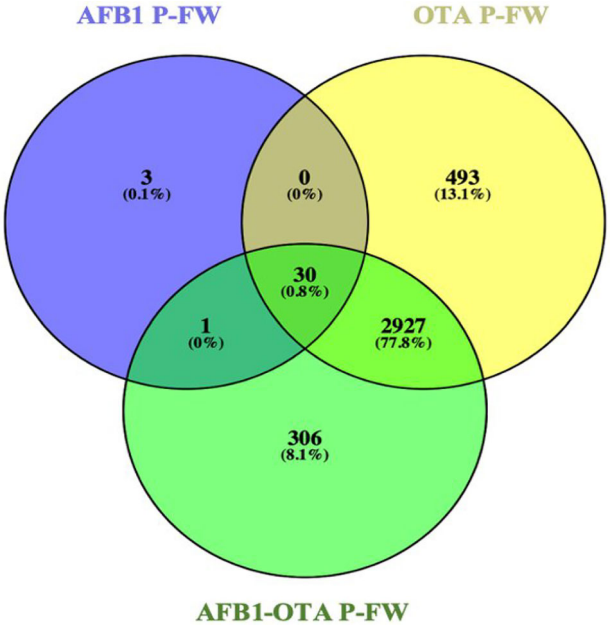

Figure 1. Venn diagram for the DEGs obtained in Jurkat cells treated during 7 days with AFB1 P-FW (196 nM), OTA P-FW (1037 nM), and AFB1-OTA P-FW (187–837 nM). DEGs with p-value ≤0.05 and log2FC |1.0|. DEGs, differentially expressed genes; FC, fold change; FW, fermented whey; P, pumpkin.

expression levels up to 32% of human genome, which contains 21 000 protein-coding genes (HGNC database). Venn diagram showed that only one DEG (UMODL1) overlapped between AFB1 P-FW and combined exposure while 2927 genes (78%) between OTA P-FW and mixed treatment (**Figure 1**). From the 30 DEGs (0.8%) overlapping in all studied conditions, 20 were upregulated and 10 downregulated, reaching log2FC values up to 4.00 in overexpression (GPR17 and TIGD5) and approximately −4.00 in repression (RHOB) (**Figure 2**).

3.2. Gene Ontology Analysis

In transcriptomics studies, a critical step is the characterization of biological processes (BP), molecular functions (MF), and cellular component (CC) by comparing the DEGs list with the rest of genome for over-represented functions and gene set enrichment analysis.[47] In relation to AFB1 P-FW exposure, DAVID analysis provided a list of GO terms in which regulation of cell morphogenesis and development were the most over-represented BP. Double-stranded DNA binding was the only MF to be statistically significant in the DEGs list while actin cytoskeleton was the unique CC significantly represented after the treatment (**Table 4**).

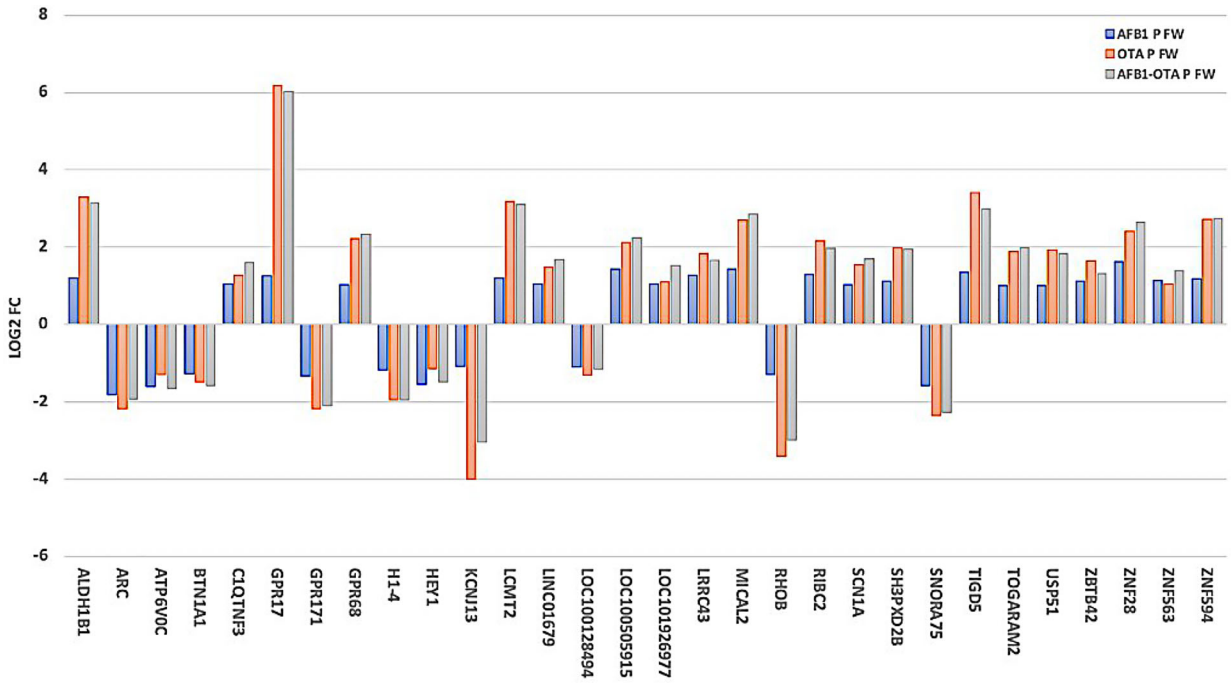

Figure 2. Log2FC values for the 30 DEGs overlapped in all studied conditions: AFB1 P-FW (196 nM), OTA P-FW (1037 nM), and AFB1-OTA P-FW (187–837 nM). DEGs with p-value ≤ 0.05 and log2FC |1.0|. DEGs, differentially expressed genes; FC, fold change; FW, fermented whey; P, pumpkin.

In OTA P-FW exposure, some of the most over-represented BP were interferon (IFN) type I signaling pathway, cellular response to cytokine, T cell differentiation, and blood vessel development. MF related to double-stranded DNA binding, chemokine, and cytokine receptor activities were statistically significant in the DEGs list. CC such as plasma membrane, ion channel complex, chromatin, and MHC protein complex were significantly affected (Table 4).

In the mixed condition, DAVID analysis showed as the regulation of adaptative immune response, immune system development, lymphocyte activation, IFN type I signaling pathway, and lymph vessel development were some of the most over-represented BP. MF linked to double-stranded DNA binding, chemokine, and cytokine receptor activities were statistically significant in the DEGs set. CC like plasma membrane, ion channel complex, MHC protein complex, and chromatin were significantly represented to a greater extent (Table 4).

3.3. PathVisio Analysis

3.3.1. AFB1 P-FW Condition

PathVisio analysis revealed a total of 3596 data points (N) and only 108 of them met criterion (R), in which (N) indicates the total number of genes measured in the dataset whereas (R) denotes the filter criterion of the analysis.[44] Numerous pathways were statistically significant after AFB1 P-FW exposure (Z-score >1.96; adj. p-value ≤ 0.05). It is interesting to observe as three different pathways of eicosanoid metabolism (via lipoxygenases, cyclooxygenases, and cytochrome P450 monooxygenases) were statistically altered with 29%, 21%, and 50% of genes affected, respectively. The analysis also showed a significant alteration in SARS coronavirus and innate immunity (17% of genes affected), PI3K/AKT/mTOR (14%), and Wnt/beta catenin (14%) signaling pathways (**Table 5**).

According to Z-score value, the most affected pathway was eicosanoid metabolism via lipoxygenases (6.39). **Figure 3** showed the genes involved, indicating in red and blue the overexpressed and downregulated, respectively. ALOX12 and ALOX15, key pathway regulators, were the most affected genes.

3.3.2. OTA P-FW Condition

The analysis conducted by PathVisio showed a total of 3696 data points, of which a large number (2557) met the criterion. Several pathways related to immune and inflammatory responses were statistically significant upon OTA P-FW treatment (Z-score > 1.96; adj. p-value ≤ 0.05). Based on the number of genes affected, all pathways showed more than 85% of genes affected. The 100% of genes involved in type I IFN induction, TRL4 signaling, SARS coronavirus and innate immunity, and development of immune cells were significantly altered (**Table 6**).

The genes associated with host–pathogen interaction of human coronaviruses induced IFN signaling (Z-score: 3.34) were showed in **Figure 4**. High fold changes values reaching up to 2.90 in overexpression (RIPK1) and −4.56 in repression (FOS) were found.

3.3.3. AFB1-OTA P-FW Condition

PathVisio assessment indicated a total of 3681 data points, of which a higher number (2413) matched the criterion. In this case,

Table 4. Relevant GOs resulted from the over-representation analysis of DEGs obtained by treatments through DAVID bioinformatics resources.

Exposure	Category	Term	Level	Count	%	*p*-Value
AFB1 P-FW						
	GO:0022604	Regulation of cell morphogenesis	BP5	4	11.8	<0.05
	GO:0060284	Regulation of cell development	BP5	5	14.7	<0.05
	GO:0003690	Double-stranded DNA binding	MF5	6	17.6	<0.01
	GO:0015629	Actin cytoskeleton	CC5	4	11.8	<0.05
OTA P-FW						
	GO:0071345	Cellular response to cytokine stimulus	BP5	207	6.0	<0.001
	GO:0030217	T cell differentiation	BP5	56	1.6	<0.001
	GO:0034340	Response to type I interferon	BP5	27	0.8	<0.01
	GO:0001568	Blood vessel development	BP5	135	3.9	<0.01
	GO:0003690	Double-stranded DNA binding	MF5	353	10.2	<0.001
	GO:0004950	Chemokine receptor activity	MF5	11	0.3	<0.01
	GO:0004896	Cytokine receptor activity	MF5	24	0.7	<0.05
	GO:0044459	Plasma membrane part	CC5	513	14.9	<0.001
	GO:0034702	Ion channel complex	CC5	66	1.9	<0.001
	GO:0000785	Chromatin	CC5	212	6.1	<0.05
	GO:0042611	MHC protein complex	CC5	10	0.3	<0.05
AFB1-OTA P-FW						
	GO:0060337	Type I interferon signaling pathway	BP5	26	0.8	<0.001
	GO:0001945	Lymph vessel development	BP5	11	0.3	<0.01
	GO:0002520	Immune system development	BP5	170	5.2	<0.01
	GO:0046649	Lymphocyte activation	BP5	135	4.1	<0.01
	GO:0002821	Regulation of immune response	BP5	26	0.8	<0.05
	GO:0003690	Double-stranded DNA binding	MF5	336	10.3	<0.001
	GO:0004950	Chemokine receptor activity	MF5	11	0.3	<0.01
	GO:0004896	Cytokine receptor activity	MF5	25	0.8	<0.01
	GO:0044459	Plasma membrane part	CC5	499	15.3	<0.001
	GO:0034702	Ion channel complex	CC5	63	1.9	<0.001
	GO:0000785	Chromatin	CC5	199	6.1	<0.05
	GO:0042611	MHC protein complex	CC5	10	0.3	<0.05

DEGs with *p*-value ≤ 0.05 and log2FC |1.0|.

Table 5. Pathways overlapped in AFB1 P-FW exposure (196 nM) by PathVisio.

Pathway	Positive (*r*)	Measured (*n*)	Total	%	Z score	Adj. *p*-value
Eicosanoid metabolism via lipooxygenases	5	17	70	29	6.39	<0.01
Eicosanoid metabolism via cytochrome P450 monooxygenases	2	4	23	50	5.51	<0.01
Eicosanoid metabolism via cyclooxygenases	3	14	70	21	4.05	<0.01
SARS coronavirus and innate immunity	2	12	33	16	2.78	<0.05
PI3K/AKT/mTOR - VitD3 signaling	2	14	34	14	2.48	<0.05
Regulation of Wnt / B-catenin signaling	2	14	33	14	2.48	<0.05

only six routes were statistically significant after the combined exposure (Z-score > 1.96; adj. *p*-value ≤ 0.05). As shown in **Table 7**, some pathways found in the individual exposures were similarly affected by the mixed condition. Also in this case, all pathways found showed more than 80% of genes affected.

Figure 5 showed the genes involved in type I IFN induction and signaling during SARS-CoV-2 infection (Z-score: 3.41). Interestingly, the alternative NF-kB pathway activation via TRAF proteins was clearly affected.

3.4. Confirmation of NGS Results by qPCR

The sequencing-based results were validated through qPCR assay. The expression of TIGD5, a DNA-binding gene, and RHOB, a Ras homolog gene, was evaluated in Jurkat cells after exposure to AFB1 P-FW, OTA P-FW, and AFB1-OTA P-FW. The experimental conditions used in qPCR analysis were the same as those used for the NGS assay. RHOB and TIGD5 were also chosen being ones of most affected genes in RNA-seq analysis. The results

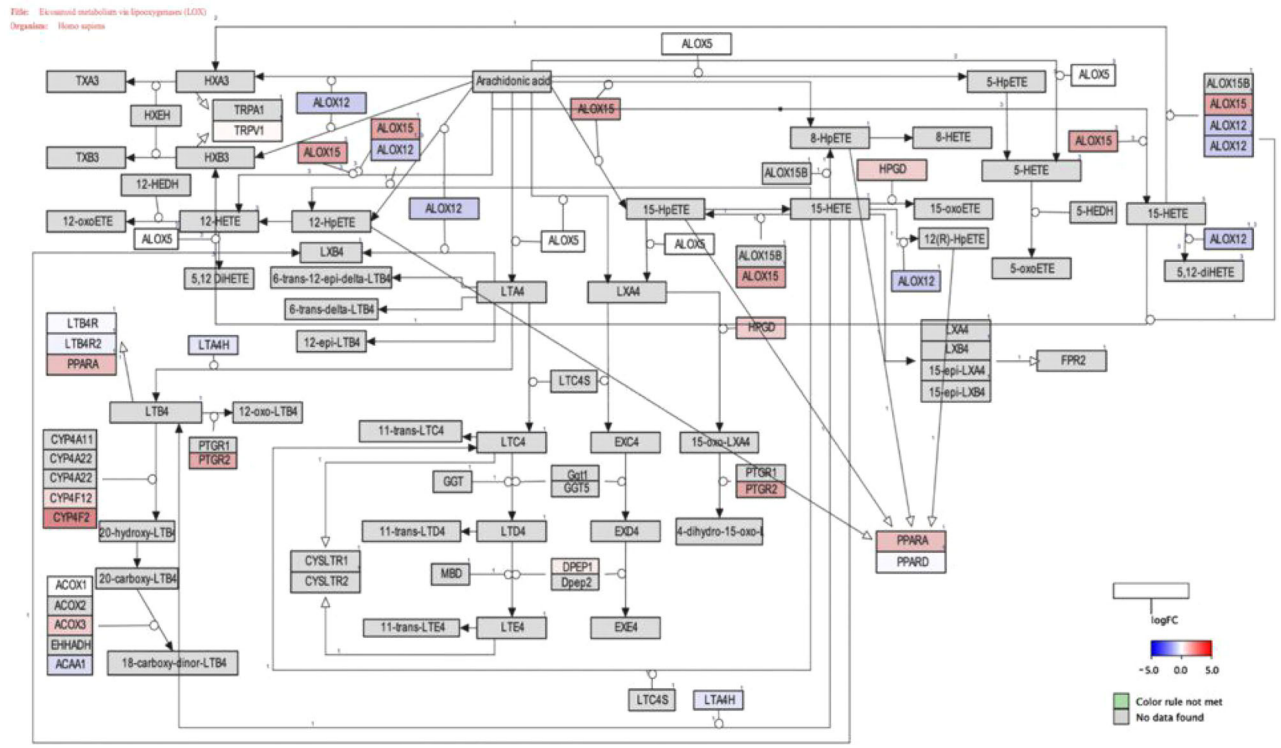

Figure 3. Genes involved in eicosanoid metabolism via lipoxygenases for Homo sapiens are shown: in red the upregulated genes and in blue the downregulated upon AFB1 P-FW exposure (196 nM). FW, fermented whey; P, pumpkin.

Table 6. Pathways overlapped in OTA P-FW exposure (1037 nM) by PathVisio.

Pathway	Positive (*r*)	Measured (*n*)	Total	%	Z Score	Adj. *p*-value
Host–pathogen interaction of human coronaviruses induced interferon signaling	30	31	47	96	3.34	<0.01
Type I interferon induction and signaling during SARS-CoV-2	22	22	45	100	3.14	<0.01
SARS coronavirus and innate immunity	13	13	33	100	2.41	<0.01
TLR4 signaling and tolerance	13	13	30	100	2.41	<0.05
Interleukin-1 structural pathway	34	40	52	85	2.18	<0.05
Toll-like receptor signaling related to MyD88	19	21	32	90	2.12	<0.05
Development of dendritic cells and macrophage subsets	9	9	14	100	2.00	<0.05

obtained were in line with NGS assay showing TIGD5 upregulation and RHOB downregulation when compared to the control (**Figure 6**). House-keeping gene GAPDH was used as endogenous gene control.

4. Discussion

In the present study, the possible beneficial effect of P-FW mixture against AFB1 and OTA induced immune toxicity was investigated at transcriptomic level. To reproduce a realistic scenario, human lymphoblastic Jurkat cells were employed, being a robust immune model to reproduce human situations in vitro.[48,49] The selected exposure time (7 days) reflects the peak of immune response in vivo, thereafter the number of T-lymphocytes decreases and the immune system gradually tends to deactivate.[50,51] Analyzing the number of DEGs following the exposure with mycotoxins and functional ingredients, it should be emphasized as only 34 DEGs were altered by AFB1, 3450 by OTA, and 3264 by combined exposure, which could exclude an additive effect between AFB1 and OTA when combined with bioactive compounds (Figure 1). The possible antagonism between mycotoxins was further confirmed by qPCR analysis (Figure 6). Likewise, our research group, using the same experimental conditions (cell line, exposure time, and digested bread extracts) for a proteomic analysis, found a lower number of differentially expressed proteins in the combined

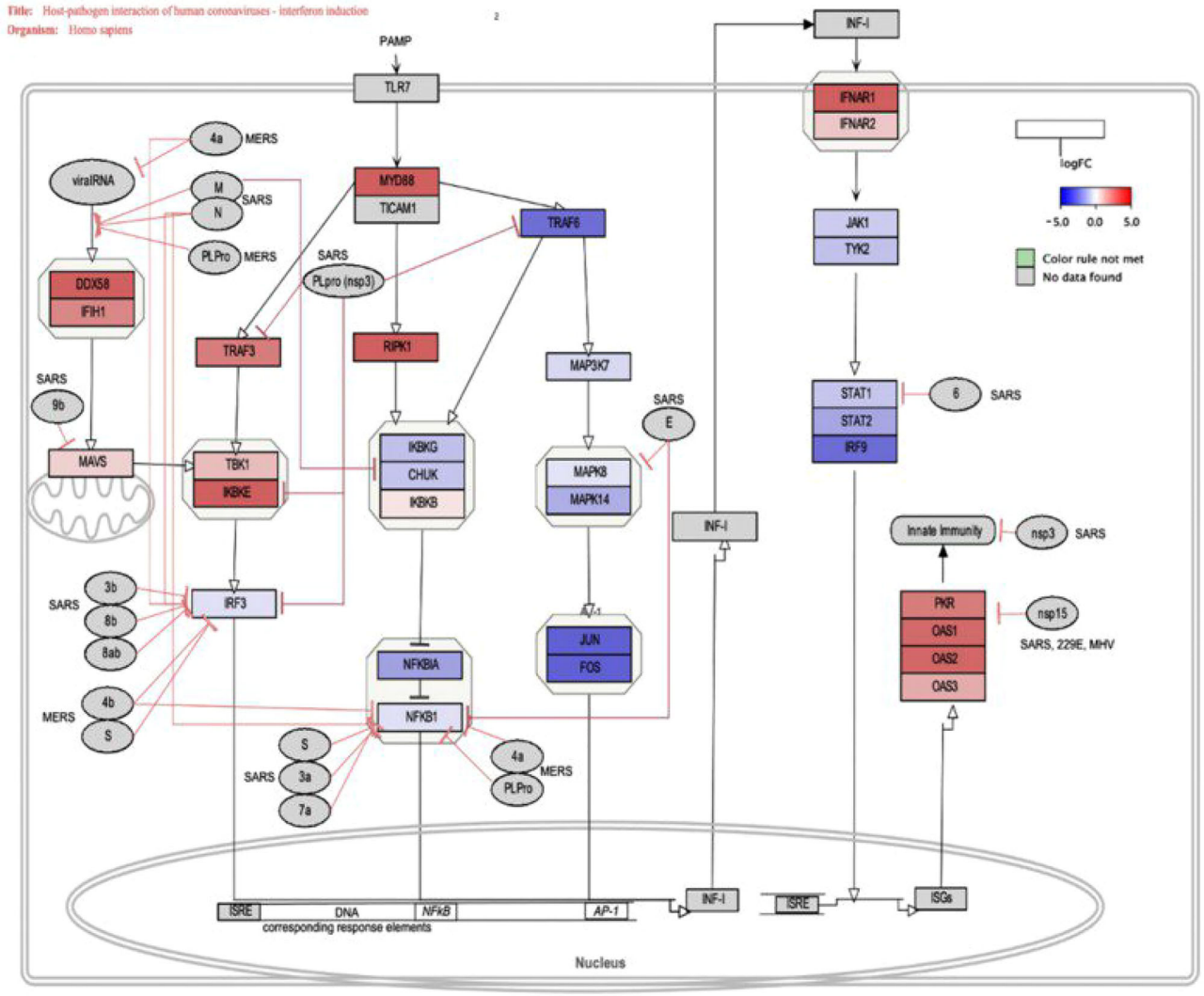

Figure 4. Genes involved in host–pathogen interaction of human coronaviruses induced interferon signaling for Homo sapiens are shown: in red the upregulated genes and in blue the downregulated after OTA P-FW exposure (1037 nM). FW, fermented whey; P, pumpkin.

Table 7. Pathways overlapped in AFB1-OTA P-FW exposure (187–837 nM) by PathVisio.

Pathway	Positive (*r*)	Measured (*n*)	Total	%	Z score	Adj. *p*-value
Type I interferon induction and signaling during SARS-CoV-2 infection	22	22	45	100	3.41	<0.01
Host–pathogen interaction of human coronaviruses - interferon induction	27	31	47	87	2.53	<0.01
SARS coronavirus and innate immunity	12	12	33	100	2.51	<0.01
Regulation of chromatid separation at the metaphase-anaphase transition	14	15	16	93	2.27	<0.05
Interleukin-1 pathway	33	40	52	82	2.27	<0.01
Eicosanoid metabolism via cyclooxygenases (COX)	12	13	70	92	2.03	<0.05

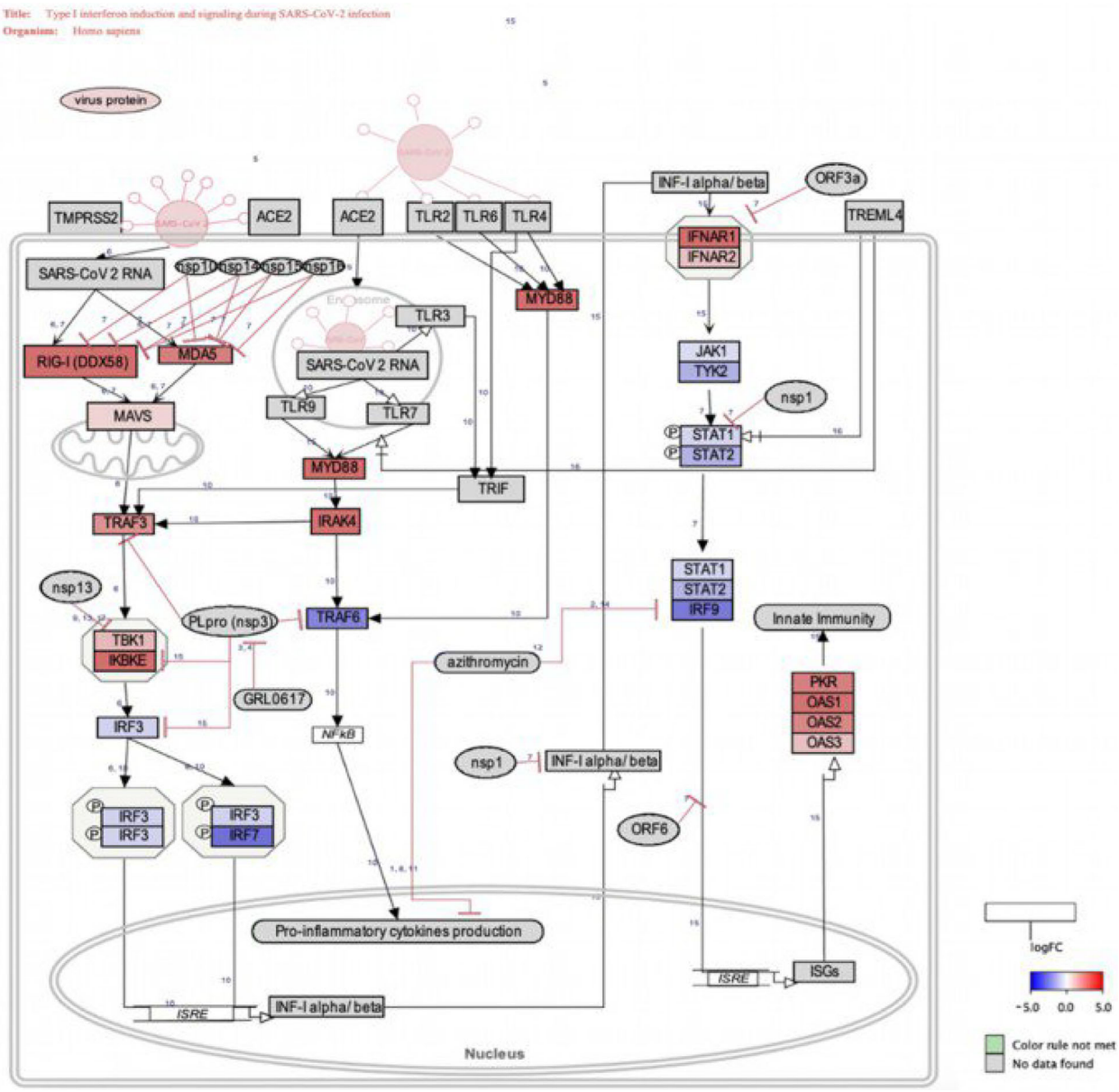

Figure 5. Genes involved in type I interferon induction and signaling during SARS-CoV2 infection for Homo sapiens are shown: in red the upregulated genes and in blue the downregulated after AFB1-OTA P-FW exposure (187–837 nM). FW, fermented whey; SARS-CoV-2, severe acute respiratory syndrome coronavirus 2; P, pumpkin.

exposure compared to the individual ones.[52] Frangiamone et al.[28] also showed an antagonist effect between AFB1 and OTA when combined with P-FW mixture treating SH-SY5Y cells ongoing differentiation during 7 days. Moreover, it is interesting to note as the mixed treatment shared 80% of DEGs with OTA individual exposure (Figure 1). These results can be related to OTA-concentration, which is almost fivefold higher than AFB1 in the mixture, and may be explained by the greater effectiveness of bioactive compounds to reduce AFB1 intestinal bioaccessibility (a reduction of 70%) compared to OTA (only 10%) in contaminated breads.[8]

Considering all studied conditions, the overlapping of 30 DEGs was obtained (Figure 2). Among them, the clear overexpression of several genes belonging to the zinc finger family (ZNF28, 563, 594), GPR17 (G protein-coupled receptor), and the downregulation of RHOB was observed. The upregulation of zinc finger proteins has been reported to attenuate NF-kB signaling activation, brain inflammatory injury, and proinflammatory cytokines production in vitro and in vivo.[53–55] Likewise, Maekawa et al.[56] revealed that GPR17 upregulation exerted inhibitory effects on inflammatory response and leukotrienes production in mouse bone marrow-derived macrophages. RHOB downregulation has been also shown to modulate TLR-mediated inflammatory response and cytokines production in macrophages, being a novel target for the treatment of inflammatory diseases.[57] In line with DAVID data analysis, in

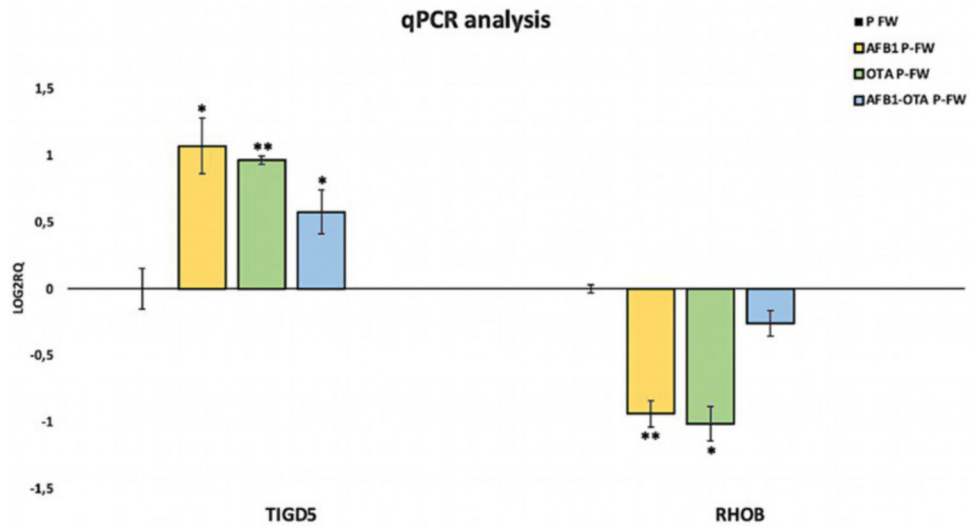

Figure 6. Bar plot showing the relative expression of TIGD5 and RHOB when compared to the control (Log2RQ = 0) after 7 days of exposure in Jurkat cells to AFB1 P-FW (196 nM), OTA P-FW (1037 nM), and AFB1-OTA P-FW (196–837 nM) by qPCR. FW, fermented whey; P, pumpkin; RHOB, Ras Homolog Family Member B; RQ, relative quantification; TIGD5, tigger transposable element derived 5. $p \leq 0.05$ (*), $p \leq 0.01$ (**).

which most DEGs were related to the immune system, these results also demonstrated a clear effect on the inflammatory response in vitro after mycotoxins and bioactive compounds exposure (Table 4). In addition, an interesting confirmation of proteomic results obtained by Cimbalo et al.[52] was the altered expression of several genes encoding for the histone family, which play a key role in maintaining genome topology. Herein, the decreased H1.4 expression was observed, which was associated with a strong induction of IFN response in vitro (Figure 2).[58]

4.1. AFB1 P-FW Exposure

Exposure to AFB1 P-FW promoted the activation of several pathways associated with eicosanoid metabolism (Table 5). Eicosanoids are lipid-based signaling molecules that play a unique role in the inflammatory response, by regulating the production of certain cytokines and chemokines.[59] Eicosanoids are also actively involved in the immune toxicity mediated by mycotoxins. For instance, AFB1-exposure (25 μM for 48 h) elicited the production of proinflammatory eicosanoids and cytokines in human macrophages, which in turn triggered the necrosis of HepG2 liver cells as well as the growth and development of hepatocellular carcinoma in vivo.[60] Similarly, the RNA-seq performed on bovine macrophages revealed the activation of eicosanoid signaling pathway and its active involvement in the immune cell death mediated by OTA-exposure (10 μM for 6 h).[61] In addition, the proteomic analysis conducted on human macrophages showed as the emerging mycotoxin alternariol (1 μM for 3 h) caused immune toxicity, by increasing the production of eicosanoids such as 12-HETE, which enhanced the transcription of proinflammatory mediators.[62] Kostro et al.[63] also demonstrated that zearalenone-induced mycotoxicosis in sheep (3.07–14.49 μg kg^{-1} for 70 days) was mediated by eicosanoids, which fostered the infiltration of neutrophils in the digestive tract and the onset of systemic inflammation.

Conversely, the use of bioactive compounds such as carotenoids, probiotics, and phenolic compounds, typically contained in P-FW mixture, has been reported to be an effective strategy in the modulation of eicosanoid production and inflammatory response.[64] Storniolo et al.[65] showed as the mixture of carotenoids and phenolic acids relieved oxidative stress and eicosanoids production in human monocytes, by promoting the resolution of inflammation and atherosclerosis disease. Likewise, a mixture of antioxidant and anti-inflammatory compounds (naturally contained in Brazilian propolis) not only modulated cytokines production but also selectively inhibited the synthesis of proinflammatory eicosanoids in vivo.[66] Pumpkin pulp also demonstrated a protective role against mycotoxins exposure in ECV304 cells (OTA, BEA, ZEA; 0.1 μM for 9 days), inhibiting the production of inflammatory eicosanoids, (prostaglandin D2 and leukotrienes B4 and E4) and protecting the integrity of blood-brain barrier in vitro.[67]

In this study, the eicosanoid metabolism via lipoxygenases was the main pathway to be altered, in which the downregulation of ALOX12 and LTA4H as well as the upregulation of ALOX15 were found (Figure 3). ALOX12 and ALOX15 are key mediators of eicosanoid production with different functions. Indeed, the strong downregulation of ALOX12 has been reported to show anti-inflammatory effects by suppressing the production of eicosanoids and pro-inflammatory cytokines in mice, pigs, and monkeys.[68] While, ALOX15 upregulation has been widely associated with the resolution of several human pathologies through the synthesis of anti-inflammatory mediators such as lipoxins.[69,70] For instance, RNA-seq performed on T98G neuroglia cells revealed the anti-inflammatory effect of functional compounds (derived from plants extracts) via ALOX12 downregulation, which in turn repressed the eicosanoid cascade. The production of anti-inflammatory lipoxins prompted by ALOX15 was also investigated.[71] Similarly, LTA4H downregulation was correlated with the anti-inflammatory response and modulation of NF-kB and eicosanoid signaling pathways activation.[59,72] In view

of this, the results obtained may confirm the beneficial protective effect of P-FW mixture against eicosanoid activation and the possible proinflammatory cascade induced by AFB1 in Jurkat cells.

4.2. OTA P-FW Exposure

The main pathway to be affected by OTA P-FW exposure was the IFN signaling (Figure 4). IFNs play a crucial role in modulating the immune response and inflammation, being produced especially during stress and infection.[73,74] Several studies have reported the close connection between IFN induction and mycotoxin toxicity.[75] Indeed, the combination of OTA and deoxynivalenol promoted the release of proinflammatory cytokines such as IL-6, IL-17, and IFN-γ in mice splenocytes. Mycotoxin exposure also caused the activation of IFN signaling pathway, which in turn stimulated the differentiation of naive T-cells into Th1/17 phenotype, increasing the susceptibility to inflammatory diseases.[76] The integrative transcriptomic and proteomic analysis carried out using differentiated Caco-2 cells demonstrated that OTA and AFM1 combined exposure (10 μM for 48 h) triggered the activation of several pathways associated with the immune and inflammatory response. A marked production of proinflammatory cytokines was also observed, leading to intestinal barrier disruption and severe gut inflammation.[77] In addition, exposure to low doses of OTA in vivo (0.5–250 μg kg^{-1} for 2–7 weeks) induced IFN signaling pathway activation and cytokines storm (TNF-α, IL-2, IL-4, and IFN-γ) resulting in liver and kidney inflammation along with intestinal dysbiosis.[78–80]

The promotion of IFN signaling pathway by which OTA induced immune toxicity and inflammation in vitro and in vivo involves the activation of several chain factors, including the overexpression of MyD88 and MAPK proteins as well as the phosphorylation and upregulation of NF-kB and JUN/FOS cascade, which in turn active AP-1 transcriptional complex, a master regulator of inflammatory response.[81–84] In the present study, although MyD88 overexpression indicated IFN pathway activation, the strong downregulation of JUN/FOS, MAPK, and NF-kB suggested a clear downstream anti-inflammatory effect of P-FW mixture against OTA in Jurkat cells (Figure 4). Similar results were obtained by Ha et al.,[85] testing a mixture of carotenoids on HaCaT cells previously treated with TNF-α and IFN-γ. The bioactive compounds showed a marked anti-inflammatory effect by reducing the production of inflammatory cytokines and inhibiting NF-kB and MAPK signaling activation. Furthermore, astaxanthin (AST) and Kefir, a fermented milk product, alleviated OTA-induced cecal injury and inflammation in mice (5 mg kg^{-1} for 21 days in both studies) downregulating the gene expression of INF-γ, NF-kB, TRL-4, and modulating the activation of several immunity-associated pathways.[86,87] In the present study, OTA P-FW exposure also led to JAK/STAT downregulation, which has been associated with the suppression of proinflammatory response in vitro and in vivo.[88–90]

4.3. AFB1-OTA P-FW Exposure

AFB1-OTA P-FW exposure triggered a transcriptional effect quite similar to OTA P-FW treatment with IFN signaling pathway activation (Figure 5). The simultaneous administration of AFB1 and OTA has been widely associated with inflammation and immune response. Corcuera et al.,[91] exposing rats to AFB1 and OTA (0.25 and 0.50 mg kg^{-1} for 0.8–96 h) obtained inflammatory infiltrates in liver and kidney tissues with cirrhosis and glomerulonephritis outbreak. Similarly, AFB1 and OTA combined exposure (0.5 and 1 μM for 48 h) promoted immune toxicity in macrophages, activating certain pathways associated with the immune response (JUN and MAPK cascade). In this case, the administration of bioactive compounds mitigated mycotoxin toxicity.[92] The RNA-seq conducted on differentiated Caco-2 cells after AFM1 and OTA combined exposure (50 and 4 μM for 48 h) also revealed transcriptional alterations in some pathways related to inflammation and immunity such as NF-kB and IFN activation. Although the number of DEGs excluded the additive effect of mycotoxins, the promotion of gut inflammation by AFM1-OTA treatment was clearly proven.[93]

Also for AFB1 OTA P-FW exposure, IFN pathway activation occurred via MyD88 overexpression, but nonetheless the involvement of additional drivers such as TRAF3, TRAF6, IRF3, and IRF7 was observed. In detail, TRAF3 was upregulated while the others drivers were downregulated (Figure 5). TRAFs are specific factors associated with TNF receptor and play a major role in the pathogenesis of inflammatory diseases.[94] Among them, TRAF3 is a tumor suppressor and a negative regulator of NF-kB alternative activation. Thus, TRAF3 overexpression has been shown to attenuate the inflammatory response in immune cells.[95] Likewise, TRAF6 downregulation can exert an inhibitory effect on NF-kB cascade and cytokine storm in mammary epithelial cells.[96] Li et al.[97] associated the anti-inflammatory effect of lycopene supplementation (5 mg kg^{-1} for 21 days) in mice with cardiac injury with TRAF6 and NF-kB downregulation. Similarly, a mixture of *Lactobacillus*, typically used for milk fermentation, relieved ZEA-inflammatory effects (25 μM for 1 h) in IPEC-J2 cells, through the downregulation of several proinflammatory markers, including TRAF-6.[98] A similar anti-inflammatory response has been reported to be mediated by IRF3 and IRF7 downregulation, two master regulators of IFN induction against pathogens infection. The RNA-seq performed on mice lungs showed that AST (20 mg mL^{-1}; 24 h) suppressed lipopolysaccharide-induced inflammation and acute lung injury through the down-regulation of 11 immune markers, including IRF7.[99] The downregulation of IRF3 and IRF7 with mitigation of IFN signaling cascade and inflammatory response was also achieved by treating fish hepatocytes and murine macrophages with high doses of AST and LAB strains, respectively.[100,101] In line with these results, our findings may further support the potential anti-inflammatory in vitro effect of P-FW mixture against AFB1-OTA combined exposure (Figure 5).

5. Concluding Remarks

This is the first transcriptomic study assessing the possible beneficial effect of P-FW mixture against AFB1 and OTA immunotoxicity in vitro, by using digested bread extracts. RNA-seq not only revealed as the majority of DEGs were correlated with the immune system and inflammatory response but also the possible antagonistic effect between AFB1 and OTA when combined with bioactive compounds. Furthermore, PathVisio analysis showed that eicosanoid pathway via lipoxygenases was the main pathway

to be altered by AFB1 P-FW. However, the modulation of several genes associated with the inflammatory response (ALOX12, ALOX15, and LTA4H) suggested the protective role of P-FW mixture against eicosanoid activation and the proinflammatory cascade prompted by AFB1 in Jurkat cells. On the other hand, exposure to OTA P-FW mainly affected IFN signaling cascade. The repression of intrinsic pathways such as NF-kB, JUN/FOS, and MAPK pointed to the strong downstream anti-inflammatory effect of P-FW mixture in vitro. In AFB1-OTA P-FW exposure, IFN signaling was again the most altered, but nonetheless the involvement of additional drivers was observed. Herein, the decreased expression of genes: TRAF6, IRF3, IRF7, and inherent pathways (NF-kB/TRAF3) typically involved in the proinflammatory response further supported the beneficial role of P-FW against the mixture of mycotoxins. Although the transcriptome analysis showed promising results, further investigations are needed to better explore the use of such food preservatives in vivo as immunomodulatory agents against AFB1 and OTA induced proinflammatory response and immune toxicity.

Acknowledgements

This work was supported by the Spanish Ministry of Science and Innovation (PID2019-108070RB-I00-ALI).

Conflict of Interest

The authors declare no conflict of interest.

Author Contributions

M.F. and M.L. contributed equally to this work.

M.F.: formal analysis, methodology, visualization, writing – original draft, writing – review. **M.L.**: formal analysis, methodology, writing – original draft. **A.C.**: formal analysis, visualization, writing – review. **A.L.**: methodology, visualization. **G.F.**: funding, supervision, writing – review, project administration. **L.M.**: conceptualization, formal analysis, methodology, supervision, writing - review, project administration.

Data Availability Statement

The data that support the findings of this study are available from the corresponding author upon reasonable request.

Keywords

bioactive compounds, inflammation, Jurkat cells, mycotoxins, RNA-sequencing

Received: December 28, 2022
Revised: April 4, 2023
Published online:

[1] S. Yin, L. Niu, Y. Liu, *Molecules* **2022**, *27*, 6141.
[2] European Commission, *Off. J. Eur. Union.* **2006**, *364*, 5.
[3] EFSA Panel on Contaminants in the Food Chain, *EFSA J.* **2020**, *18*, e06113.
[4] C. Luz, F. Saladino, J. Mañes, G. Meca, *Rev. de Toxicol.* **2018**, *35*, 106.
[5] E. Sarmast, A. A. Fallah, T. Jafari, A. M. Khaneghah, *Curr. Opin. Food Sci.* **2021**, *39*, 68.
[6] B. Kabak, F. Ozbey, *J. Food Compos. Anal.* **2012**, *27*, 21.
[7] W. Simla, S. Porasuphatana, P. Songsermsakul, *J. Pharm. Sci.* **2009**, *5*, 108.
[8] L. Escrivá, F. Agahi, P. Vila-Donat, J. Mañes, G. Meca, L. Manyes, *Toxins* **2022**, *14*, 6.
[9] F. Saladino, E. Posarelli, C. Luz, F. B. Luciano, M. T. Rodriguez-Estrada, J. Mañes, G. Meca, *J. Food Compos. Anal.* **2018**, *68*, 128.
[10] C. H. Versantvoort, A. G. Oomen, E. Van de Kamp, C. J. Rompelberg, A. J. Sips, *Food Chem. Toxicol.* **2005**, *43*, 31.
[11] R. Assunção, C. Martins, D. Dupont, P. Alvito, *Food Chem. Toxicol.* **2016**, *96*, 205.
[12] C. Luz, J. Ferrer, J. Mañes, G. Meca, *Food Chem. Toxicol.* **2018**, *112*, 60.
[13] D. D. Chaplin, *J. Allergy Clin. Immunol.* **2010**, *125*, S3.
[14] L. Manyes, G. Font, in *Encyclopedia of Human Nutrition*, 4th ed., Elsevier, New York, NY **2022**. https://doi.org/10.1016/B978-0-12-821848-8.00147-5
[15] Y. Sun, Y. Song, M. Long, S. Yang, *Toxins* **2023**, *15*, 187.
[16] M. Viljoen, N. Claassen, *J. Hazard. Mater.* **2023**, *9*, 100228.
[17] M. Frangiamone, M. Lozano, A. Cimbalo, G. Font, L. Manyes, *Foods* **2023**, *12*, 259.
[18] M. Gavahian, N. Pallares, F. Al Khawli, E. Ferrer, F. J. Barba, *Trends Food Sci. Technol.* **2020**, *106*, 209.
[19] C. Bergantin, A. Maietti, P. Tedeschi, G. Font, L. Manyes, N. Marchetti, *Molecules* **2018**, *23*, 2791.
[20] C. Gupta, D. Prakash, *Beverages* **2017**, *3*, 31.
[21] A. Sadeghi, M. Ebrahimi, M. Raeisi, S. M. Ghods Mofidi, *J. Food Meas. Charact.* **2019**, *13*, 2837.
[22] C. Luz, L. Izzo, A. Ritieni, J. Manes, G. Meca, *Lwt* **2020**, *118*, 108717.
[23] L. Escrivá, L. Manyes, P. Vila-Donat, G. Font, G. Meca, M. Lozano, *Food Funct.* **2021**, *12*, 11250.
[24] C. Juan, D. Montesano, J. Mañes, A. Juan-García, *J. Funct. Foods* **2022**, *92*, 105049.
[25] M. Alonso-Garrido, M. Frangiamone, G. Font, A. Cimbalo, L. Manyes, *Food Chem. Toxicol.* **2021**, *153*, 112261.
[26] M. Frangiamone, A. Cimbalo, G. Pérez, M. A. Garrido, L. Manyes, *Rev. de Toxicol.* **2021**, *38*, 1.
[27] F. Illueca, P. Vila-Donat, J. Calpe, C. Luz, G. Meca, J. M. Quiles, *Toxins* **2021**, *13*, 752.
[28] M. Frangiamone, M. A. Alonso-Garrido, G. Font, A. Cimbalo, L. Manyes, *Food Chem. Toxicol.* **2022**, *164*, 113011.
[29] E. Y. Agarkova, A. G. Kruchinin, O. A. Glazunova, T. V. Fedorova, *Nutrients* **2019**, *11*, 2930.
[30] C. Ji, L. Yan, Y. Chen, S. Yue, Q. Dong, J. Chen, M. Zhao, *J. Hazard. Mater.* **2019**, *368*, 514.
[31] A. Cimbalo, M. Frangiamone, G. Font, L. Manyes, *Food Chem. Toxicol.* **2022**, *169*, 113396.
[32] S. Andrews, FastQC: A Quality Control Tool for High Throughput Sequence Data **2020**. http://www.bioinformatics.babraham.ac.uk/projects/fastqc/
[33] G. J. Hannon, FASTX-Toolkit **2010**. http://hannonlab.cshl.edu/fastx_toolkit
[34] A. Dobin, C. A. Davis, F. Schlesinger, J. Drenkow, C. Zaleski, S. Jha, T. R. Gingeras, *Bioinform.* **2013**, *29*, 15.
[35] H. Li, B. Handsaker, A. Wysoker, T. Fennell, J. Ruan, N. Homer, R. Durbin, *Bioinform.* **2009**, *25*, 2078.
[36] R. C. Team, R: A Language and Environment for Statistical Computing **2018**.

[37] M. D. Robinson, D. J. McCarthy, G. K. Smyth, *Bioinform.* **2010**, *26*, 139.
[38] L. Escrivá, D. Jennen, F. Caiment, L. Manyes, *Toxicol. Lett.* **2018**, *284*, 213.
[39] M. Alonso-Garrido, L. Escrivá, L. Manyes, G. Font, *Food Chem. Toxicol.* **2018**, *121*, 437.
[40] R. Kolde, pheatmap: Pretty Heatmaps. R package version 1.0. 12. CRAN. R-project. org/package = pheatmap **2019**.
[41] J. Swinton, Vennerable Package **2013**. https://github.com/js229/Vennerable
[42] D. W. Huang, B. T. Sherman, R. A. Lempicki, *Nucleic Acids Res.* **2009**, *37*, 1.
[43] D. W. Huang, B. T. Sherman, R. A. Lempicki, *Nat. Protoc.* **2009**, *4*, 44.
[44] M. Kutmon, M. P. van Iersel, A. Bohler, T. Kelder, N. Nunes, A. R. Pico, C. T. Evelo, *PLoS Comput. Biol.* **2015**, *11*, e1004085.
[45] M. Martens, A. Ammar, A. Riutta, A. Waagmeester, D. N. Slenter, K. Hanspers, M. Kutmon, *Nucleic Acids Res.* **2021**, *49*, D613.
[46] S. A. Bustin, V. Benes, J. A. Garson, J. Hellemans, J. Huggett, M. Kubista, C. T. Wittwer, *Clin. Chem.* **2009**, *55*, 611.
[47] A. Conesa, P. Madrigal, S. Tarazona, D. Gomez-Cabrero, A. Cervera, A. McPherson, A. Mortazavi, *Genome Biol.* **2016**, *17*, 1.
[48] J. Shao, L. F. Berger, P. J. Hendriksen, A. A. Peijnenburg, H. van Loveren, O. L. Volger, *Arch. Toxicol.* **2014**, *88*, 673.
[49] C. Cassioli, S. Balint, E. B. Compeer, J. H. Felce, A. Gamberucci, C. Della Bella, C. T. Baldari, *Front. Cell Dev. Biol.* **2021**, *9*, 673446.
[50] V. P. Badovinac, B. B. Porter, J. T. Harty, *Nat. Immunol.* **2002**, *3*, 619.
[51] N. A. Lieberman, V. Peddu, H. Xie, L. Shrestha, M. L. Huang, M. C. Mears, A. L. Greninger, *PLoS Biol.* **2020**, *18*, e3000849.
[52] A. Cimbalo, M. Frangiamone, M. Lozano, L. Escrivá, P. Vila-Donat, L. Manyes, *World Mycotoxin J.* **2022**, *1*, 165.
[53] J. Y. Hong, W. Bae, J. K. Yi, G. T. Kim, E. C. Kim, *J. Periodont. Res.* **2016**, *51*, 529.
[54] J. Zhan, W. Qin, Y. Zhang, J. Jiang, H. Ma, Q. Li, Y. Luo, *J. Neuroinflamm.* **2016**, *13*, 1.
[55] R. Agnihotri, S. Gaur, *Sci. World J.* **2022**, *2022*, https://doi.org/10.1155/2022/4612054
[56] A. Maekawa, B. Balestrieri, K. F. Austen, Y. Kanaoka, Proc. Natl. Acad. Sci. **2009**, *106*, 11685.
[57] N. Zhang, L. Fu, Y. Bu, Y. Yao, Y. Wang, *Mol. Immunol.* **2017**, *91*, 42.
[58] N. Serna-Pujol, M. Salinas-Pena, F. Mugianesi, F. Le Dily, M. A. Marti-Renom, A. Jordan, *Nucleic Acids Res.* **2022**, *50*, 3892.
[59] A. E. Sheppe, M. J. Edelmann, *Infect. Immun.* **2021**, *89*, e00095.
[60] A. Fishbein, W. Wang, H. Yang, J. Yang, V. M. Hallisey, J. Deng, D. Panigrahy, *Proc. Natl. Acad. Sci. USA* **2020**, *117*, 21576.
[61] K. M. Brennan, S. Y. Oh, A. Yiannikouris, D. E. Graugnard, N. A. Karrow, *Toxins* **2017**, *9*, 366.
[62] G. Del Favero, R. M. Mayer, L. Dellafiora, L. Janker, L. Niederstaetter, C. Dall'Asta, D. Marko, *Cells* **2020**, *9*, 847.
[63] K. Kostro, K. Dudek, U. Lisiecka, B. Majer-Dziedzic, R. Aleksiewicz, K. Lutnicki, *Bull. Vet. Inst. Pulawy* **2012**, *56*, 75.
[64] A. Kamalian, M. Dolatshahi, K. Afshari, S. Shamshiri, N. M. Roudsari, A. H. Abdolghaffari, *World J. Gastroenterol.* **2020**, *26*, 3365.
[65] C. E. Storniolo, I. Sacanella, M. T. Mitjavila, R. M. Lamuela-Raventos, J. J. Moreno, *Nutrients* **2019**, *11*, 1880.
[66] J. C. Ferreira, M. B. Reis, G. D. Coelho, G. H. Gastaldello, A. P. F. Peti, D. M. Rodrigues, K. F. Zoccal, *J. Ethnopharmacol.* **2021**, *278*, 114255.
[67] M. Alonso-Garrido, N. Pallarés, G. Font, P. Tedeschi, L. Manyes, M. Lozano, *Arh. Hig. Rada Toksikol.* **2021**, *173*, 173.
[68] X. J. Zhang, X. Liu, M. Hu, G. J. Zhao, D. Sun, X. Cheng, H. Li, *Cell Metab.* **2021**, *33*, 2059.
[69] N. K. Singh, G. N. Rao, *Prog. Lipid Res.* **2019**, *73*, 28.
[70] R. G. Snodgrass, Y. Benatzy, T. Schmid, D. Namgaladze, M. Mainka, N. H. Schebb, B. Brüne, *Cell Death Differ.* **2021**, *28*, 1301.
[71] A. Panossian, E. J. Seo, T. Efferth, *Phytomedicine* **2019**, *60*, 152881.
[72] Z. Wei, Y. Liu, M. Yang, M. Li, K. Li, L. Zheng, S. Yang, *Biocell* **2021**, *45*, 1005.
[73] F. J. Barrat, M. K. Crow, L. B. Ivashkiv, *Nat. Immunol.* **2019**, *20*, 1574.
[74] J. M. Rojas, A. Alejo, V. Martín, N. Sevilla, *Cell. Mol. Life Sci.* **2021**, *78*, 1423.
[75] M. Frangiamone, A. Cimbalo, M. Alonso-Garrido, P. Vila-Donat, L. Manyes, *Food Chem. Toxicol.* **2022**, *160*, 112798.
[76] S. Jahreis, S. Kuhn, A. M. Madaj, M. Bauer, T. Polte, *Food Chem. Toxicol.* **2017**, *109*, 405.
[77] Y. Gao, Q. Ye, X. Bao, X. Huang, J. Wang, N. Zheng, *Toxicon* **2020**, *180*, 49.
[78] D. E. Marin, G. C. Pistol, M. Gras, M. Palade, I. Taranu, *Naunyn-Schmiedeb. Arch. Pharmacol.* **2018**, *391*, 1147. https://doi.org/10.1007/s00210-018-1538-9
[79] K. Prasanna, A. K. Sharma, P. Dwivedi, C. C. Satheesh, A. G. Telang, Indian J. Sci. Res. **2007**, *31*, 1.
[80] W. Wang, S. Zhai, Y. Xia, H. Wang, D. Ruan, T. Zhou, L. Yang, *Microbiome* **2019**, *7*, 1.
[81] H. Xu, S. Hao, F. Gan, H. Wang, J. Xu, D. Liu, K. Huang, *Chem. Biol. Interact.* **2017**, *272*, 107.
[82] R. Kumar, S. Alam, B. P. Chaudhari, P. D. Dwivedi, S. K. Jain, K. M. Ansari, M. Das, *Carcinogenesis* **2013**, *34*, 647.
[83] F. Gan, Y. Zhou, L. Hou, G. Qian, X. Chen, K. Huang, *Chemosphere* **2017**, *182*, 630.
[84] P. Wan, S. Zhang, Z. Ruan, X. Liu, G. Yang, T. Jia, J. Wu, *Virulence* **2022**, *13*, 502.
[85] Y. Ha, W. H. Lee, J. Jeong, M. Park, J. Y. Ko, O. W. Kwon, Y. J. Kim, *Nutrients* **2020**, *12*, 1238.
[86] Y. Chen, S. Zhao, D. Jiao, B. Yao, S. Yang, P. Li, M. Long, *Oxid. Med. Cell. Longev.* **2021**, *2021*. https://doi.org/10.1155/2021/8894491
[87] G. Du, S. Chang, Q. Guo, X. Yan, H. Chen, K. Shi, T. Yue, *Int. Food Res. J.* **2022**, *158*, 111551.
[88] C. D. Mohan, C. Kim, K. S. Siveen, K. A. Manu, S. Rangappa, A. Chinnathambi, K. S. Ahn, *IUBMB Life* **2021**, *73*, 1348.
[89] J. Kowshik, A. B. Baba, H. Giri, G. Deepak Reddy, M. Dixit, S. Nagini, *PLoS One* **2014**, *9*, e109114.
[90] A. Salas, C. Hernandez-Rocha, M. Duijvestein, W. Faubion, D. McGovern, S. Vermeire, N. Vande Casteele, *Nat. Rev. Gastroenterol. Hepatol.* **2020**, *17*, 323.
[91] L. A. Corcuera, A. Vettorazzi, L. Arbillaga, E. Gonzalez-Peñas, A. L. De Cerain, *Food Chem. Toxicol.* **2012**, *50*, 3440.
[92] L. Hou, F. Gan, X. Zhou, Y. Zhou, G. Qian, Z. Liu, K. Huang, *Chemosphere* **2018**, *199*, 718.
[93] Y. N. Gao, X. Yang, J. Q. Wang, H. Liu, N. Zheng, *Toxins* **2022**, *14*, 368.
[94] A. I. Lalani, S. Zhu, S. Gokhale, J. Jin, P. Xie, *Curr. Pharmacol. Rep.* **2018**, *4*, 64.
[95] J. Zhang, T. Chen, X. Yang, H. Cheng, S. S. Späth, P. E. Clavijo, C. Van Waes, *Cancer Res.* **2018**, *78*, 4613.
[96] X. P. Wang, Z. M. Luoreng, L. S. Zan, F. Li, N. Li, *J. Dairy Sci.* **2017**, *100*, 7648.
[97] X. N. Li, J. Lin, J. Xia, L. Qin, S. Y. Zhu, J. L. Li, *J. Funct. Foods* **2017**, *29*, 208.
[98] I. Taranu, D. E. Marin, G. C. Pistol, M. Motiu, D. Pelinescu, *Toxicon* **2015**, *97*, 53.
[99] K. Mao, W. Geng, Y. Liao, P. Luo, H. Zhong, P. Ma, Y. Jin, *Aging* **2020**, *12*, 18716.
[100] H. Fang, J. Xie, W. Zhao, Z. Liu, Y. Liu, L. Tian, J. Niu, *Aquac. Nutr.* **2021**, *27*, 2575.
[101] Z. Cai, P. Xu, Z. Wu, D. Pan, *J. Funct. Foods* **2018**, *51*, 16.